

# Litho-Lineament Mapping of Rocks in Ila Orangun Area Southwestern Nigeria Using Remote Sensing and Aeromagnetic Data: Implications for Mineral Exploration

Jayeola, A.O.<sup>1</sup>, Ayodele O. S<sup>2</sup>., Akinluyi, F.O.<sup>2</sup>, Balogun, O. B<sup>3</sup>

<sup>1</sup>Department of Earth Sciences, Adekunle Ajasin University, Akungba Akoko, Ondo State, Nigeria.

<sup>2</sup>Department of Applied Geology, The Federal University of Technology, Akure, Ondo State, Nigeria.

<sup>2</sup>Department of Remote Sensing and Geoinformatics Science, The Federal University of Technology, Akure, Ondo State, Nigeria.

<sup>3</sup>Department of Geosciences, Mountain Top University, Prayer City, Ogun State, Nigeria.

doi : <https://doi.org/10.37745/bjesr.2013/vol12n11341>

Published February 13, 2024

---

**Citation:** Jayeola, A.O., Ayodele O. S., Akinluyi, F.O., Balogun, O. B (2024) Litho-Lineament Mapping of Rocks in Ila Orangun Area Southwestern Nigeria Using Remote Sensing and Aeromagnetic Data: Implications for Mineral Exploration, British Journal of Earth Sciences Research, 12 (1),13-41

---

**ABSTRACT:** *Ila Orangun is located north of Okemesi and falls within latitudes 7°54' and 8°00' N and longitudes 4° 53' and 5° 00' E respectively. Field studies revealed six lithological units in the study area namely quartzites, granites, granite gneiss, porphyritic granites, amphibolite schist and pegmatites. The aim of the research is to elucidate the geology and structure as well as evaluate the metallic mineral potentials of the study area. An integrated multi-technique study approach was adopted for reconnaissance survey and structural interpretation which involved the use of acquired remotely sensed satellite imageries such as Landsat-8 OLI, Shuttle Radar Topographic Mission, Radar Sentinel-2A and a geophysical method involving the use of aeromagnetic data. Results obtained from interpretation of remote sensing data was used to produce different lineament maps which displayed fractures of varying lengths and trend dominantly in the NE-SW directions and subsidiary fractures also orientate in the NW-SE, E-W and N-S directions. Results from the stereographic projection plots showed that the dominant orientation of foliation planes is in the NE-SW direction with the NE and SE sections of the study area recording the highest cluster of the foliation planes. Hence, the eastern section spotted as the mineralization zone.*

**KEYWORDS:** Ila Orangun, Remote sensing, Lineament, Aeromagnetic data, Brittle

---

## INTRODUCTION

The study area, Ila Orangun falls within the basement complex of southwestern Nigeria. It is noted to be the headquarter of Ila Local Government Area in the present-day Osun State. The

study area occupies an area of about 143.745 km<sup>2</sup> between 7° 54' and 8° 001' N latitude and between 4° 53' and 5° 00' E longitude. However, with the continuously growing availability of geoscience data acquired by field and remote sensing methods, there is an increasing demand to interpret and analyze such multivariate data sets in a spatially consistent and integrated manner. Surveying techniques that are relevant to earth scientists include geological, geochemical, geomorphological and geophysical field surveys. These surveying techniques have over the previous centuries proven to be highly suitable in complementing conventional geological mapping, identifying targets for mineral and hydrocarbon exploration (Drury, 1992) and there is increasing awareness that they provide invaluable information to monitor the environment (Bennett and Doyle, 1997). Increasingly however, the goal of the earth scientist in investigating a region of interest is to integrate and spatially link all the available data to gain insight into the geological phenomena and processes in a study area. The line of reasoning is that each data type potentially provides complementary information and that if such data are adequately integrated more insight in the geology of an area is better understood. The use of remote sensing and Geographic Information System (GIS), Image Processing System (IPS) and other image processing accessories and software is fast gaining importance in the repertoire of field - based earth scientists which is now routinely employed in geological exploration, natural hazard and environmental applications (Drury,1992; Bonham - Carter, 1994). GIS as an exploration tool in field mapping projects are found very useful and dependent on the accessibility and terrain conditions which is very expensive in exploration and mapping programs. Hence, it is suggestable that GIS should be extended from its usual traditional application of analyzing and predicting specific phenomena, such as the presence of mineral deposits to the use of multiple data sets analysed to gain insight in the underlying geological processes. GIS and Remote Sensing becomes the vehicle by which geologists complement and enhance their inherent ability to think and unravel absolutely the geology of an area (Drury, 1992). The objective of this research was to integrate the results of lineaments obtained from the integrated remote sensing study approach involving the use of Landsat-8 OLI, Shuttle Radar Topographic Mission (SRTM) and Radar Sentinel -2A to detect possible mineralization zones.

### **The Study Area: Accessibility, Topography, Drainage and Climate**

The study area and its' environ is located within the Ilesha schist belt on a merged map sheet of Ilorin SE (Sheet No. 223) and Ilesha NE (Sheet No. 243). It is located between Latitudes 7°54' and 8° 001'N and Longitudes 4°53' and 5°00'E covering a total estimated area of about 143.745km<sup>2</sup>. The study area lies within Osun State in the Southwestern part of Nigeria (Figure 1). It is the gateway to both Ekiti and Kwara States and share boundaries with Ora Igbomina and Oke Ila to the North East; Agbamu, Arandun, Omuo-Aran to the North; Oyan to the west; Otan-Ayegbaju to the southwest and Okemesi in Ekiti State to the east. Ila Orangun township is accessible through major roads from Ora Igbomina junction, Otan-Ayegbaju, Ikirun and Ajababa. The study area is accessible through network of all seasonal roads and motorable tracks which links it with neighboring states like Ekiti and Kwara States (Figure 2)

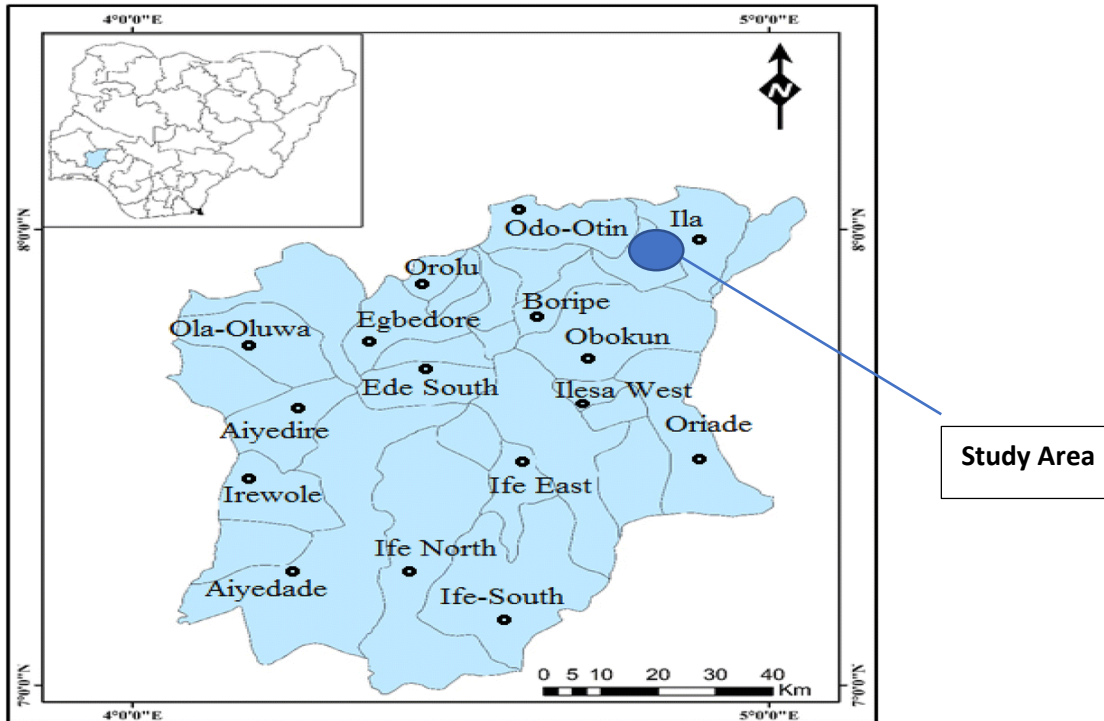


Figure 1: Map of Osun State showing the study area (Inset: Map of Nigeria)

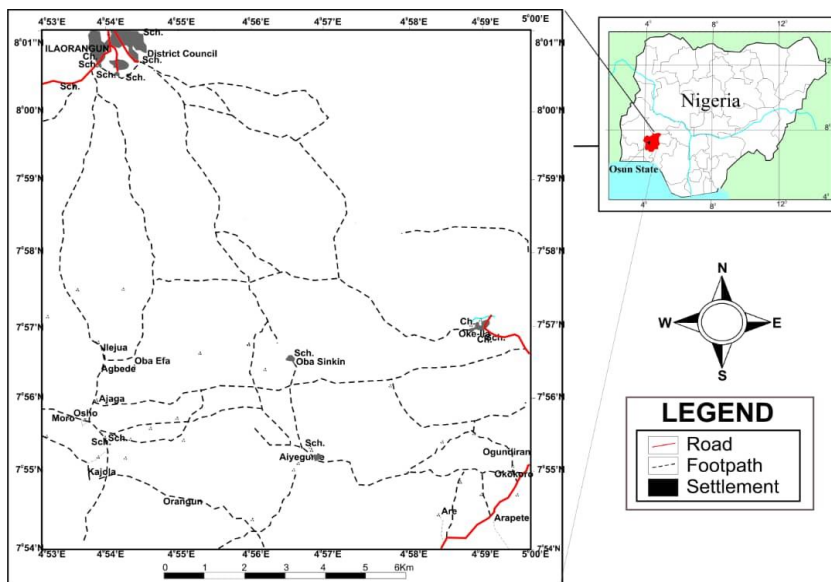
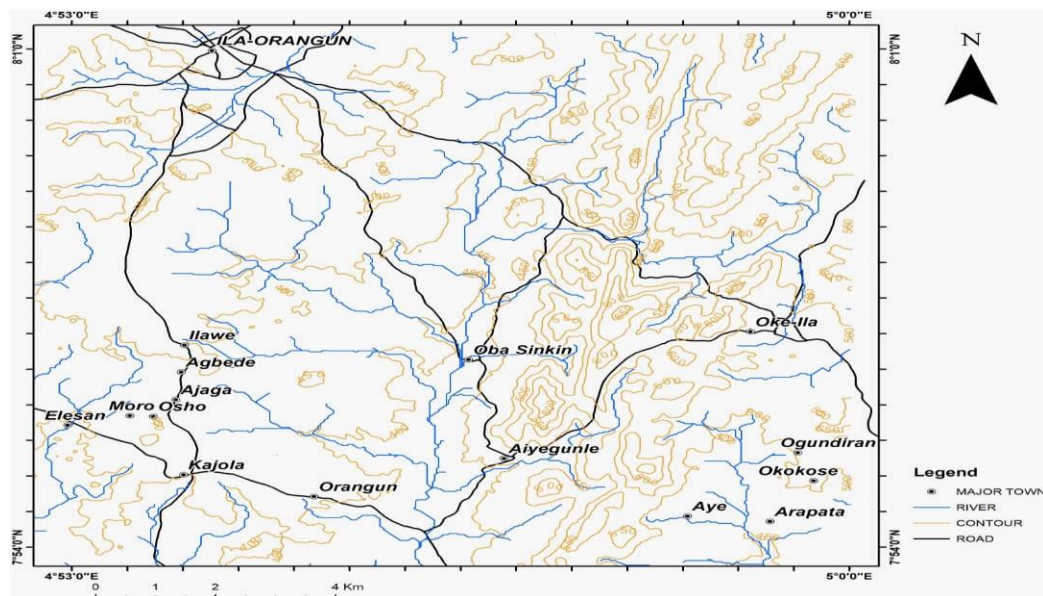


Figure 2: Interconnectivity and accessibility map of the study area (Inset: Map of Nigeria)

The topography being the general relief and landform that is peculiar to the study area depicts a rugged terrain characterized by high ranging hills with very high elevations. Hence the study area is an expression of both undulating hills which are almost flat in certain areas and plains

dotted with different outcrops in several parts. Most of the outcrops in the study area are well exposed, existing in-situ as low lying and very tall massive hills forming ridges and high mountain ranges. These massive hills were observed to dominate the entire eastern (north eastern and southeastern) parts of the area which was observed to be the most difficult terrain because of the rugged nature (Figure 3). Rocks forming long range of massive ridges in the eastern parts were observed to be dominant around Aiyegunle, Obasinkin, Obebe, Obalumo and Oke Ila which are relatively higher with heights ranging between 450m - 650m above sea level. The western parts of the area exhibit scanty outcrops as the rock exposures are generally lowlying and has no hills forming ridges.



**Figure 3: Digitized topographical map sheet of the study area on a scale of 1:50,000 (Federal Surveys Nigeria 1966, Sheet No. 223 & 243 merged)**

The major river in the study area is River Oyi with its various tributaries flowing around the various villages, hamlets and farm settlements spotted within the area. Various sections of River Oyi are seen traversing Ila Orangun and its environs as river channels bearing lowlying outcrops. The river was observed to be flowing mostly in the NE-SW directions with the river course being moderately wide and taking its tributaries from the Ayikinugba water falls. Its width is estimated to being almost 15meters during the raining season and an estimated depth of about 5meters during this season. The drainage pattern in the south-eastern part of the area where topography is dominated by series of ridges is the trellis type which suggests that the drainage here is structurally controlled whereas, the drainage pattern in other parts of the study area is dendritic, due to homogeneity of the rocks. (Figure 4).

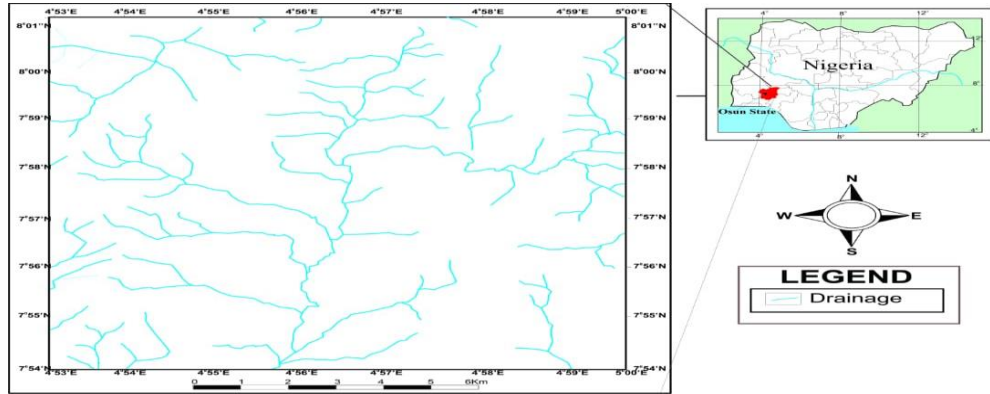


**Figure 4: Drainage map of the study area**

Ila Orangun falls within the tropical rain forest and has a humid tropical climate characterized by distinct wet and dry seasons. The wet season extends mostly between March and October while the dry season lasts between November and February. This area has an average temperature of about 29°C (Figure 5). The vegetation is generally depicted by moist deciduous forest. Due to the relatively high rainfall experienced annually the vegetation is thicker and more luxuriant. The forests are made up of different species of trees typical of the semi deciduous forest. The western part of the study area is characterized by savannah tree vegetation such as the bamboo and other wet species of trees are also found along the banks of streams and rivers. The vegetation in some parts are mainly shrubs which are used as grazing are for herbivores (Figure 6).

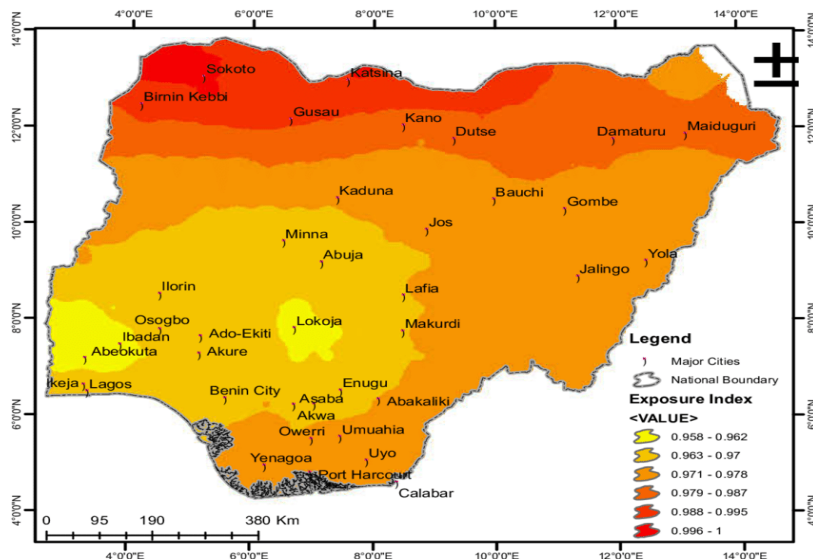


**Figure 5: Map of Nigeria showing climate distribution (Source: NIMET, 2022)**

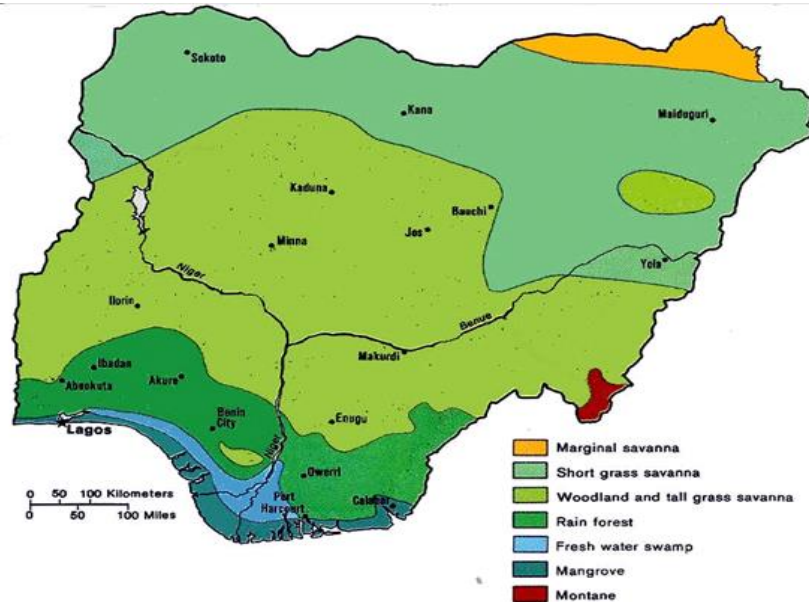


**Figure 6: Map of Nigeria showing vegetation types (Source: NIMET, 2022)**

### Local Geologic Settings

The local geology of the area shows six (6) lithological units however dominated by quartzites (massive and schistose). Other lithological units include granite, porphyritic granites, granite gneiss, pegmatites and the amphibolite green schist (Figure 7). Though the most common rock in the area is the quartzite which was observed to be widely distributed within the eastern section of the study area. Quartzites, both massive and schistose were observed around Aiyegunle, Obasinkin, Obalumo and Obebe while quartzites spotted around Aba Agbonore and Aba Jagi was seen to be very massive, extensive enough and covering a natural space of about 3km. Hence, forming a very difficult terrain with an elevation of about  $\pm 650$  meters above mean sea level. The quartzites were seen to also extend to parts of Oke-Ila as you ascend uphill from Oyi Aiyegunle to Ayikinugba all within Ifedayo Local Government area. The heavy presence of these quartzite ridges of varying heights around Obasinkin, Aba Aromodana, Aba Jagi, Aba Agbonore, Aba Obalumo and Oke Ila all in the northeastern section of the study area according to the researcher can be described as forming the **'Ila Orangun Massive Quartzite Group'**. The pegmatites spotted in Obasinkin were suspected to be intrusives which are younger than the quartzites found within the locality. The western part of the study area was seen to be characterized with scanty low-lying outcrops mainly granite gneiss, amphibolite schists, low lying quartzites, lateritic concretions common within Ila Orangun township indicating highly weathered rocks for which mineral attributes and structural features have been severely eroded. Generally, the rocks in the study area are mostly of the granitic and metamorphic origins. Thus, on the basis of its' regional geology belong to the Precambrian basement rocks of southwestern Nigeria, which itself is part of the basement rocks of Nigeria.

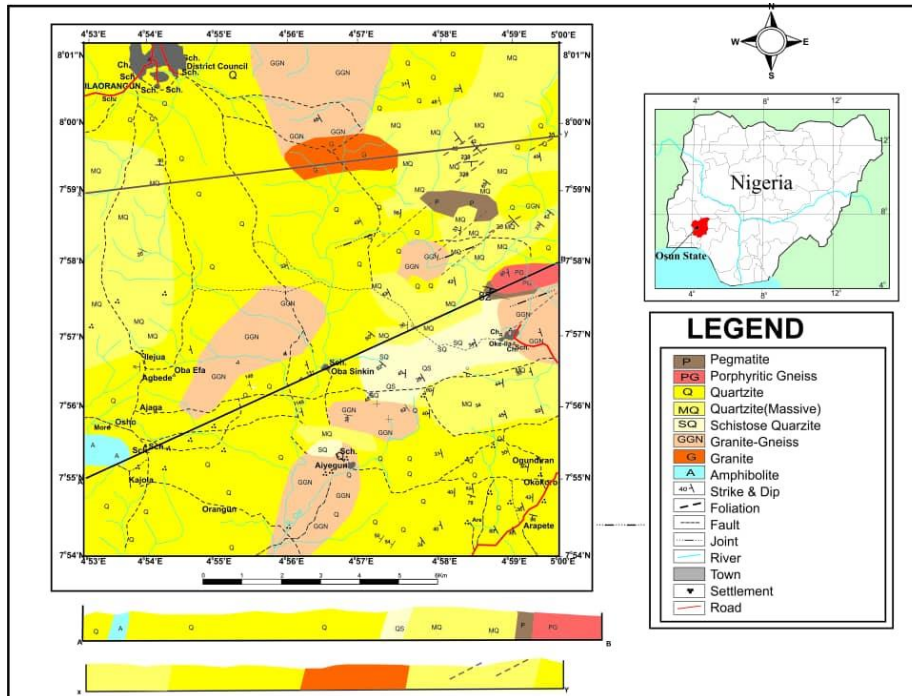


**Figure 7: Geological Map of the study area with cross sections**

## MATERIALS AND METHODS

Remote sensing materials and tools used include the Landsat -8 OLI, Shuttle Radar Sentinel -2A, Radar Sentinel -2A and geophysical methods involving the aeromagnetic and radiometric data acquired from the Nigerian Geological Survey Agency (NGSA) in 2023. However, the aeromagnetic and radiometric data of the study area contain sheet number 223 (Ilorin SE) and sheet number 243 (Ilesha NE) respectively, Other accessory tools used for the purpose of lineament extraction include Geosoft-Oasis Montaj, Open Street Mapping (OSM), ArcMap 10.3, ArcGIS 10.2, PCI Geomatica (2015 version), RockWorks 15, Surfer 10, Grapher and other software packages. This research involved acquisition and the use of relevant satellite data such as Landsat and other remotely sensed satellite imageries. Hence, for the purpose of this study, the use of remote sensing tools such as Radar Sentinel -2A, Shuttle Radar Topographic Mission (SRTM), Open Street Mapping (OSM), Digital Elevation Model (DEM) data with spatial resolution of 30m and Landsat 8 image that covers the entire study area were fully put into use. These data are then being projected to WGS 1984 UTM Zone 31 N. Then several pre- processing techniques such as conversion to top of the atmosphere reflectance, sun angle correction and layer stacking were applied on Landsat 8 data before further image processing procedures. The processing of the remote sensing datasets then followed immediately which was used to produce the various remotely-sensed satellite imageries of the study area so as to validate strange and unknown landscape characteristic features. Image processing techniques that were adopted include the Principal Component Analysis (PCA), False Colour Composition (FCC) which were all applied to the Landsat 8 data to enhance lithological discrimination while for structural interpretation, filtering and edge detection

techniques were applied to DEM to pick structural features in the form of lineaments in the study area.

## RESULTS AND DISCUSSION

The imageries shown below are those produced from Landsat -8 OLI, SRTM, Radar Sentinel -2A and a geophysical method involving the use of aeromagnetic data. Maps produced from the various remote sensing tools and the geophysical data reveal similar features which depicts and describe the general landforms and topography of the area as it showcased a rugged terrain in some sections. However, these integrated method and study approach was found useful in litho-lineament mapping and in describing the general structural trend on the various rocks.

### Hill Shade

From the hill shading produced, the images depict a 3-dimension perspective of the elevation maps produced for the study area. The essence of producing this black and white imagery of the study area is to clearly show the true topography and the general landform that characterizes the area mapped. Since aerial photograph show limitations because of their dependence on natural east-west solar illumination paths which highlight north-south linear features perpendicular to the solar illumination; therefore, hill shade generated from Digital Elevation Models (DEMs) are an alternative source for identification of lineaments. The rugged topography indicating the presence of a hilly terrain is more conspicuous on the eastern (i.e. northeastern and southeastern) section of the study area is assumed to have been the most deformed and thus affected by severe tectonic events which are evident in the large numbers of lineaments picked from this part of the study area (Figures 8 - 12).

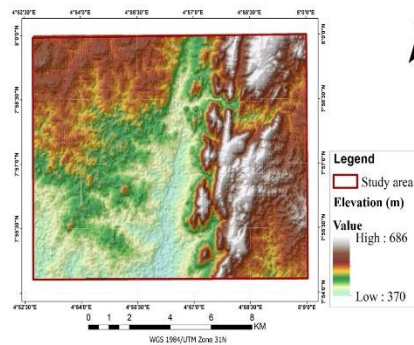
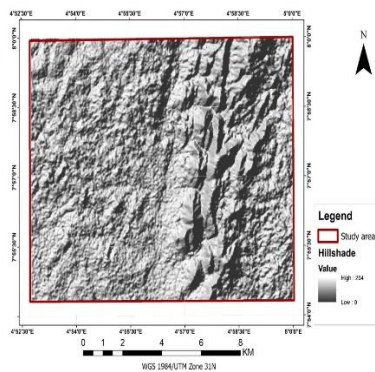


Figure 8: DEM Hillshade of the study area from SRTM

Figure 9: SRTM Coloured Digital Elevation Image of the study area



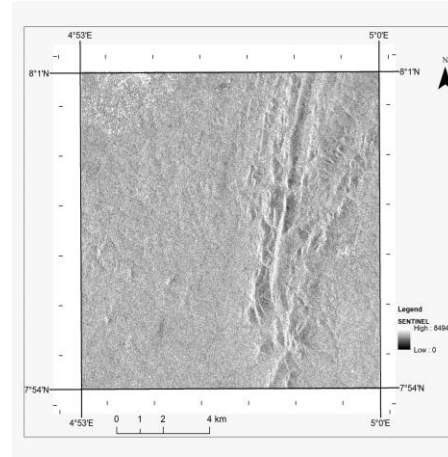
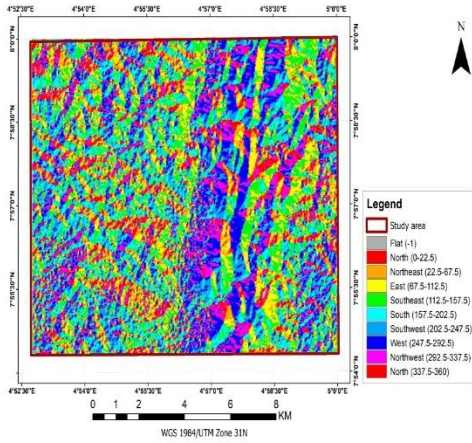


Figure 10: Aspect Ratio of the study area from SRTM Figure 11: DEM Hillshade image of the study area from Radar Sentinel - 2A

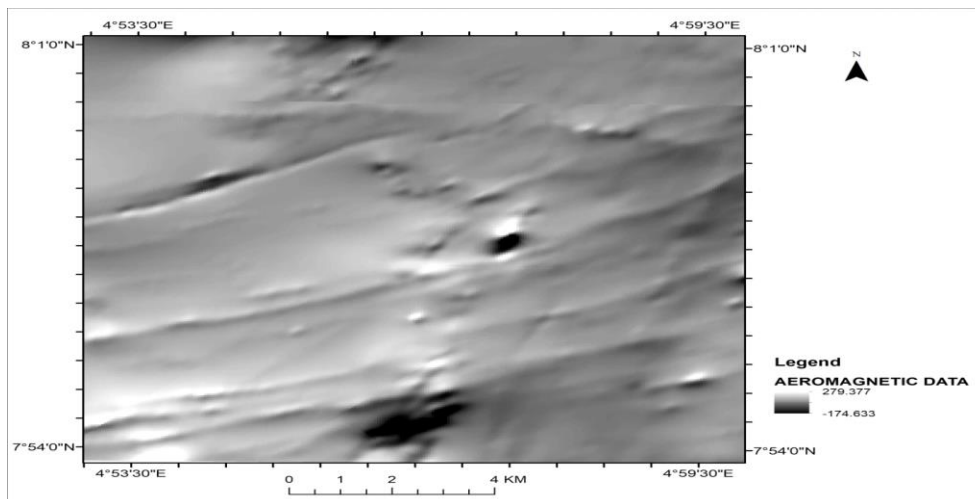


Figure 12: Raw Aeromagnetic image of the study area

### Lineament Mapping

Lineaments are described as simple or composite linear features that are aligned in a rectilinear or slightly curvilinear relationship and which differ from the adjacent features and presumably represent the subsurface phenomenon (O’Leary et al.,1976). However, three methods were applied in the study to map filled fractures and faults in the form of lineaments which involved basically the extraction of lineaments from Landsat -8, Shuttle Radar Topographic Mission (SRTM) and Radar Sentinel -2A while the use of aeromagnetic data being a geophysical method was also employed in producing lineament maps and images for the area to allow for comparison. The images below show lineament maps and the results obtained from all the remote sensing tools used for the purpose of lineament extraction and their rose diagram plots for the entire study area. Lineaments were annotated and their lengths and orientations were measured separately for different lithologies observed in the study area. The lineaments were seen occurring as being parallel to each other or in some cases crossing the next or forming an

intersection while they are found distributed across the entire study area. Important to note that in most cases reveals the intensity and density of fractures on the rock types that forms basically the underlying lithology of the area. From the lineament maps, areas with quartzites as most dominant rock type are more fractured, thus displaying greater numbers of lineaments because of the brittle nature of this rock type. Results of lineament mapping obtained from the Landsat -8 OLI data show that about 87 lineaments were captured from the study area. The lineaments were observed to be distributed across the entire study area showcasing various lengths described as short, medium and very long lineaments. Some were found crossing each other either depicting a T-crossing, X-crossing and in some cases running parallel to each other. T-crossing lineaments were observed in L8 & L9, L38 & L39 and L74 & L75. X-crossing is observed in L28 & L29 and L85 & L86 while lineaments running parallel to each other were observed in L22 & L23, L34 & L35 and L80 & L81. However, from the lineament map produced from Landsat -8 data, longer length lineaments are observed on the eastern section of the study area with lengths estimated at about 3.5cm (2.3km), 4.7cm (3.1km) and 3.0cm (2km) among others with this section of the study area on the lineament map showing conspicuously intersecting each other (T-crossing & X-crossing) and parallel lineaments too (See Appendix). Hence, a pointer to the presence of quartzites as the underlying lithology of the section because of its brittle nature and are thus capable of responding to the effects of deformational forces (Figure 13).

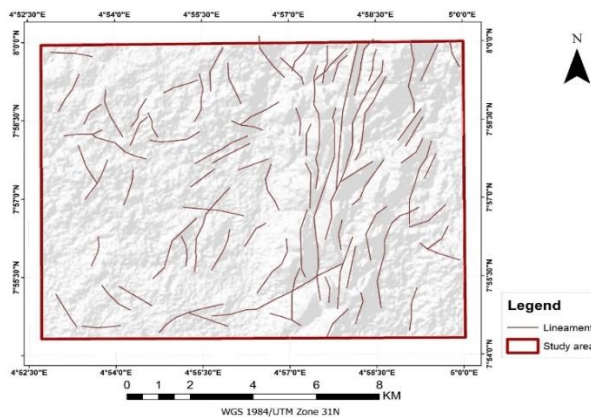


Figure 13: Landsat -8 OLI lineament Map image of the study area

Lineament mapping using the Shuttle Radar Topographic Mission (SRTM) data show a total of 19 lineaments which recorded the least number of lineaments extraction compared to those of Landsat -8 and Radar Sentinel -2A. This few numbers of lineaments captured are linked to the capacity of the SRTM remote sensing tool. Lineaments captured as seen on this map are concentrated around the eastern (northeastern and southeastern) section of the area. Lineaments of varying lengths were captured as they depict short, medium and long lineament types. Lineaments L5 & L6 were seen to form X-crossing relationship, L17 & L18 almost forming a T-crossing while L3 was observed to run parallel to L8. L7 & L8 also running parallel to each other (See Appendix). Lengths of lineaments were estimated as 3cm(2km), 2.5cm(1.6km) and 0.7cm(0.5km). From the lineament maps from SRTM, it implies that the presence of lineaments

in the eastern section of the study area was made possible because of the brittle nature of the underlying lithology of the area identified from ground truthing as quartzite. Hence, the heavy presence of lineaments in this area is a pointer to obvious effect of deformation and shearing with the cluster being an indicator for the possibility of spotting a mineralisation zone (Figure 14)

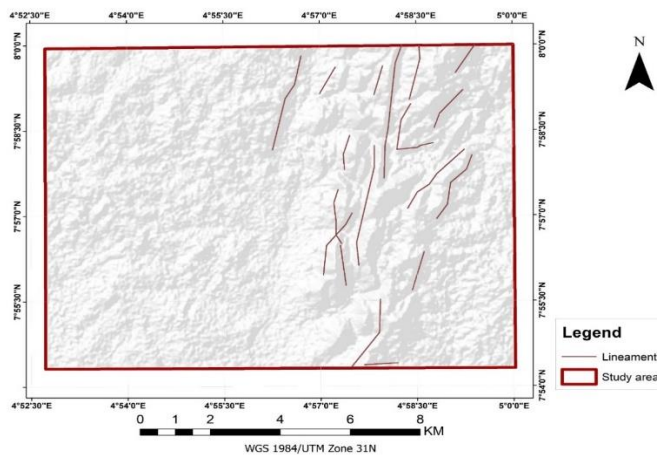


Figure 14: SRTM lineament map image of the study area

Results from the lineament mapping produced from Radar Sentinel displayed about 500 lineaments being the highest volume or population of lineament captured among all the lineament maps produced using the Landsat -8, SRTM and the Radar Sentinel -2A as remote sensing tools adopted for this research. The population of lineament captured was possible because of the capacity of the Radar Sentinel -2A to interact very well with both rocks, soils and also penetrate vegetations for maximum lineament capturing. This justifies the advantage of the Radar Sentinel -2A over Landsat -8 and SRTM. The lineaments are however, short or medium in lengths but the population of lineaments show more cluster in the eastern section of the study area with most of the lineaments crossing each other forming a T-crossing or X-crossing relationship. It is observed that the orientation of the various lineaments within the area from the Radar Sentinel show lineaments of multi directional trends as they trend in the NE-SW, NW-SE and other subsidiary lineaments trending in the N-S and E-W directions respectively (Burke et al.,1976). Hence, these lineaments favour mineralisation within the study area with more attention on the eastern section where there is high presence or density of lineaments forming cluster (Figure 15)

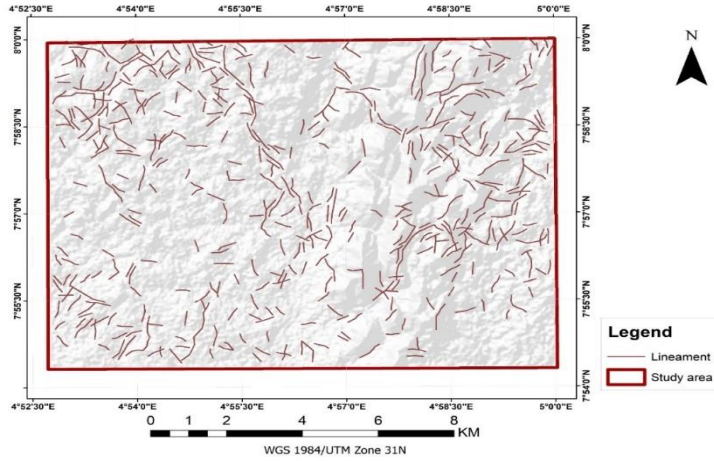


Figure 15: Radar Sentinel -2A lineament map image of the study area

Results of lineament mapping from aeromagnetic data, revealed the total number of lineaments captured as 74 and observed as having a maximum variable length that can reach 5km and an average variable length of 1.4km. Rose diagram of lineaments highlights two fracture systems, which are oriented in the NE-SW and E-W (Figure 4.11). The NE-SW fracture system has the predominant trends in the study area with the E-W system being weakly represented.

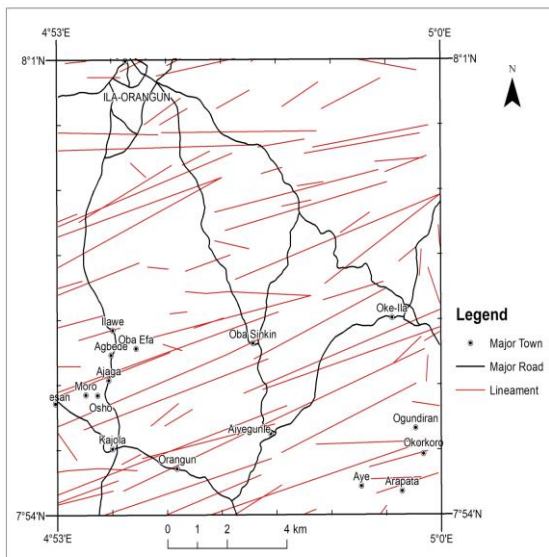


Figure 16: Lineament map of the study area extracted from aeromagnetic data (automatic)

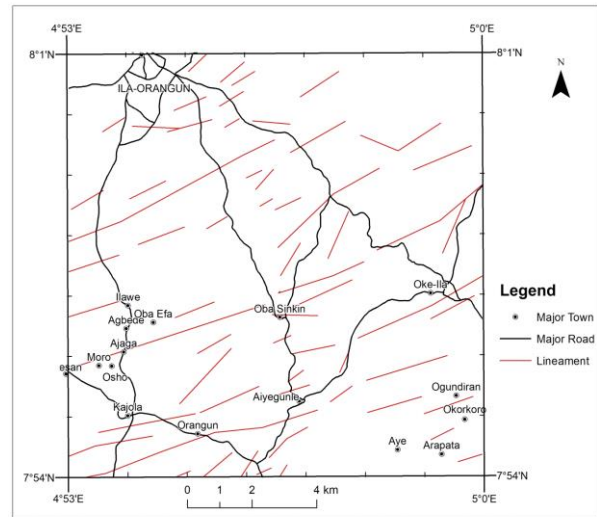


Figure 17: Lineament Map of the study area extracted manually from aeromagnetic data

Data obtained from the satellite imagery produced for the study area display automatically extracted lineaments with their lengths on imagery (cm), actual length (km), bearing and trend per lineament. The lineament map produced using a scale of 1cm to represent 1km was closely examined as each linear features (lineaments) clearly captured using satellite were subjected to measurements. The length of each visible lineament was measured in centimetres and

converted to its equivalent length in kilometres. Their bearings in degrees were carefully determined which corresponds with their direction or orientation as displayed on the extracted lineament map (Figures 11&12). The satellite imagery in this case automatically extracted about 93 lineaments with variable length that reaches up to 6-10km and an average variable length of 2.59km. Rose diagram of these lineaments shows two principal fracture systems with orientations NE-SW and E-W (Figures 4.24). We note a remarkable dominance of the NE-SW but a less dominance in the E-W systems. Below is a summary of the data obtained as a result of lineaments extracted automatically from aeromagnetic data showing azimuth, frequency, actual length (km), percentage frequency (%f) and percentage length (% l) which are thus presented for interpretation. From table 1 below a total of 93 lineaments were extracted in all with the frequency (i.e., no of occurrence) of lineaments ranging from 1 to 35. It was observed that 2 lineaments fall within azimuth 1°- 10°, 1 of the lineaments fall within azimuth 11°- 20°, 3 fall within azimuth 41°- 50°, 12 fall within azimuth 51°- 60°, 35 fall within azimuth 61°- 70°, 23 fall within azimuth 71°- 80°, 16 fall within azimuth 81°- 90°, with 1 falling within azimuth 91°- 100°. However, the total length of lineaments captured automatically is estimated at about 199km (Table 1). While the summarized data obtained from the lineaments extracted manually from aeromagnetic data showing Azimuth, Frequency, Actual length (km), Percentage frequency (%f) and Percentage length (% l) for lineaments captured for interpretation revealed a total of 74 lineaments were extracted in all with the frequency (i.e., no of occurrence) of lineaments ranging from 1 to 31. It was observed that 7 lineaments fall within azimuth 21°-30°, 3 of the lineaments fall within azimuth 31°- 40°, 3 fall within azimuth 31°- 40°, 6 fall within azimuth 41°-50°, 16 fall within azimuth 51°-60°, 31 fall within azimuth 61°-70°, 8 fall within azimuth 71°-80°, with one falling within azimuth 81°-90° and 2 of the lineaments falling within azimuth 91°-100°. However, the total length of lineaments captured manually is estimated at about 88.8km (Table 2).

**Table 1: Summarized data for lineaments extracted from aeromagnetic data(automatic)**

Azimuth (Degree)	Frequency (f)	Actual length (km)	% Frequency	% Length
1-10	2	0.9	2.15	0.45
11-20	1	1.0	1.00	1.00
21-30	-	-	-	-
31-40	-	-	-	-
41-50	3	2.3	3.22	1.15
51-60	12	21.0	12.9	10.5
61-70	35	85.8	37.6	43.1
71-80	23	55.6	24.7	27.9
81-90	16	31.8	17.2	15.9
91-100	1	0.6	1.00	0.30
101-110	-	-	-	-
111-120	-	-	-	-
121-130	-	-	-	-
131-140	-	-	-	-
141-150	-	-	-	-
151-160	-	-	-	-
161-170	-	-	-	-
171-180	-	-	-	-
<b>TOTAL</b>	<b>ΣF = 93</b>	<b>ΣL = 199km</b>	<b>Σ(%F) = 100%</b>	<b>Σ(%L) =100%</b>

**Table 2.: Summarized data for lineaments extracted from aeromagnetic data(manual)**

<b>Azimuth (Degree)</b>	<b>Frequency (f)</b>	<b>Actual length (km)</b>	<b>% Frequency</b>	<b>% Length</b>
1-10	-	-	-	-
11-20	-	-	-	-
21-30	7	5.9	9.45	6.64
31-40	3	2.1	4.05	2.36
41-50	6	7.8	8.10	8.78
51-60	16	15.3	21.6	17.2
61-70	31	41.4	41.9	46.6
71-80	8	12.9	10.8	14.5
81-90	1	1.2	1.00	1.35
91-100	2	2.2	2.70	2.47
101-110	-	-	-	-
111-120	-	-	-	-
121-130	-	-	-	-
131-140	-	-	-	-
141-150	-	-	-	-
151-160	-	-	-	-
161-170	-	-	-	-
171-180	-	-	-	-
<b>TOTAL</b>	<b><math>\Sigma F = 74</math></b>	<b><math>\Sigma L = 88.8\text{km}</math></b>	<b><math>\Sigma(\%F) = 100\%</math></b>	<b><math>\Sigma(\%L) = 100\%</math></b>

However, figures 25a-d below show rose diagrams plotted to display the lineaments extracted from the various rock types that defines the underlying lithology of the study area. Rose diagram was plotted per lithologic type so as to unveil the distribution and density of lineament on each rock type. However, the orientations of the lineaments were obtained with their lengths shown with the aid of rose diagrams (Figures 19, 21, 23 and 25a-d). Result showed that 80% of the lineaments captured from the remotely sensed satellite imagery were found on the quartzites while the remaining 20% were found on other rock types which include granite gneiss, pegmatites and amphibolites green schist. Though observation from field work showed that pegmatites and amphibolites green schist occurred as intrusions within the study area as the area is well dominated by quartzites. Comparison between the methods used for visually interpreted extracted lineaments, lineament maps produced show that more lineaments were captured from both Radar Sentinel -2A and the aeromagnetic data imageries than that of the Landsat -8 and SRTM imageries which allowed for comparison by the researcher as most of the lineaments depicting structures in the form of small fractures, faults, foliations and lineations as they exhibit varying lengths. However, it is important to note that the combination of both Landsat -8, SRTM, Radar Sentinel -2A and aeromagnetic dataset allow for adequate comparison on the basis of results obtained from such lineament analysis conducted on the study area. The area is highly deformed, as the heavy presence of lineaments were observed mostly on the quartzites lithology either massive or schistose. However, it was deduced that

the heavy presence, cluster and density of lineaments on this lithology is an indication that this rock type have been deformed with the quartzites being the most common and dominant rock type in the area. Hence, evidence of deformation is as a result of the tectonic activities that affected the area. The responses of these rocks to tectonic forces are as a result of their brittle nature, hence prone to fractures while less lineament density was only spotted on the granite.

### Lineament Density

Lineament density is a product of the total length of all recorded lineaments divided by the area under consideration which can be used to generate a lineament density map for the area under study. The density map then reveals the population of lineaments captured with reference to their distributions on the different lithologies identified in the various sections within the study area. Higher density of lineament density favours mineralization and groundwater potentials. The even distribution of the lineaments as displayed on the lineament density map is a result of the dominance of quartzites in the area which are known to be brittle. Hence, showing the most fractured lithology depicted by the population and density of lineaments captured using Landsat -8, SRTM and Radar Sentinel -2A (Figures 18, 20, 22 and 24). However, most of the lineaments on Landsat, SRTM and Radar Sentinel imageries show orientations trending towards the northeastern, northwestern and a few trending in the north-south and east-west directions. From all the three lineament density maps produced using Landsat -8 OLI, SRTM and Radar Sentinel data, areas within the study area with very high density of lineaments appear in reddish-brown colour brown colour for high density, yellow for moderate lineament density while low and very low appear in light green and deep green respectively. It therefore geologically implied that areas with very high lineament density in reddish brown colours are spots of attraction to a mineral explorationist as these are identified as the mineralisation zones within the study area especially on the eastern part. From ground truthing it was observed that the elevation values in the eastern part of the study area range between 365 and 683 meters above sea level.

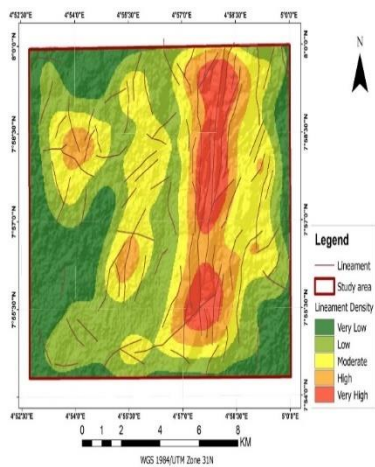


Figure 18: Lineament Density Map of the extracted from Landsat -8 OLI

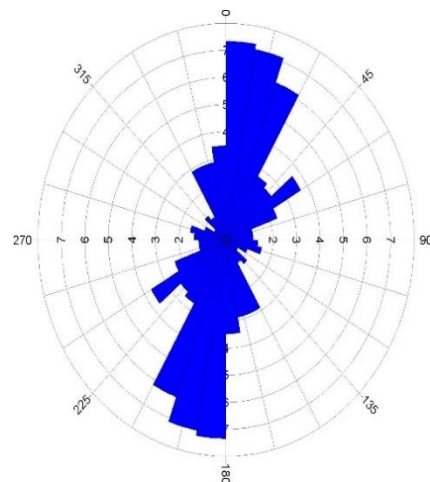


Figure 19: Rose diagram plot for lineaments extracted from Landsat -8 OLI

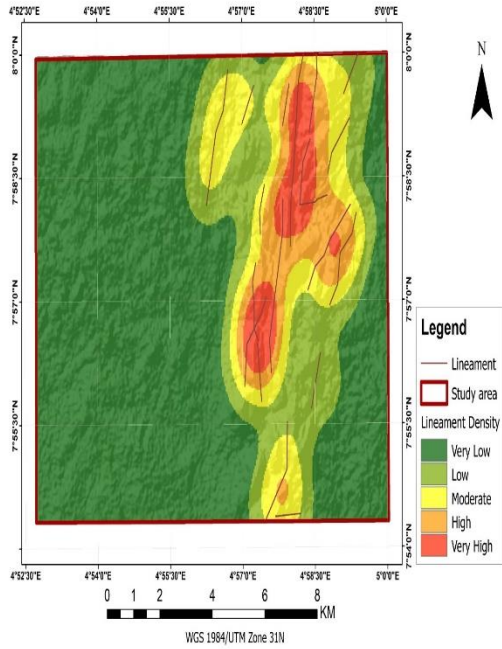


Figure 20: Lineament Density Map of the study area

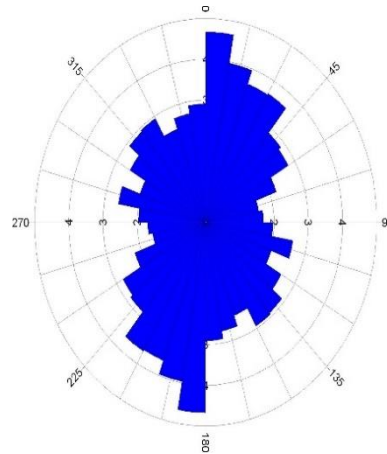


Figure 21: Rose diagram plot for lineaments extracted from SRTM

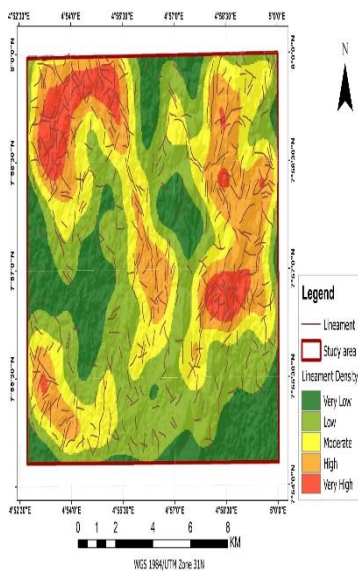


Figure 22: Lineament Density Map of the study area from Radar Sentinel -2A

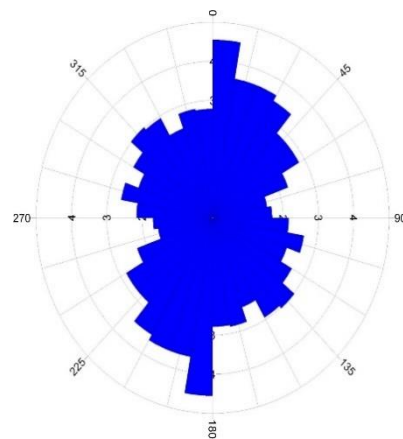


Figure 23: Rose diagram plot for lineaments extracted from Radar Sentinel -2A



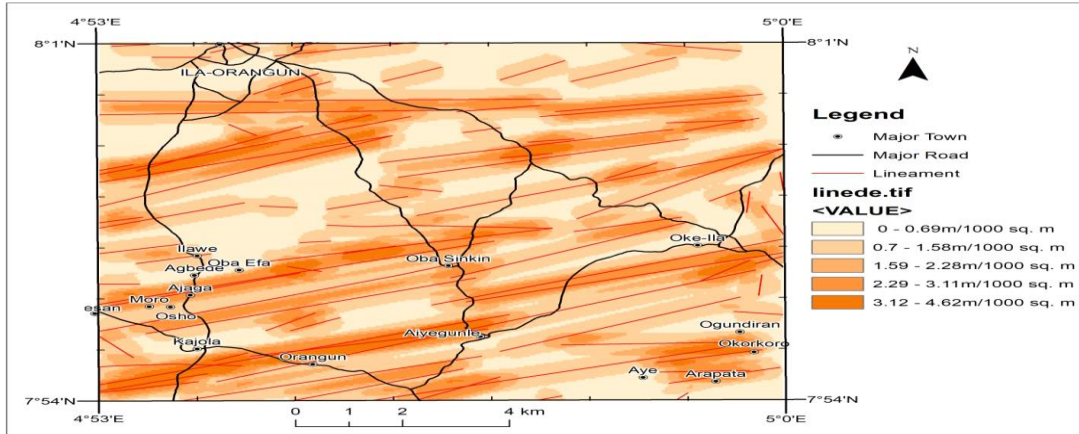
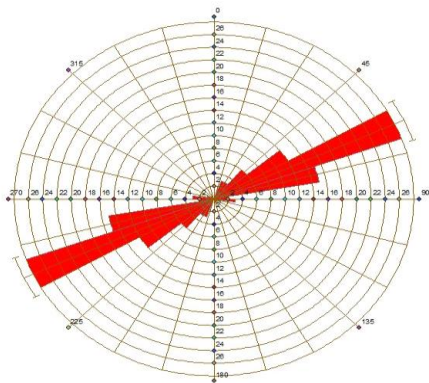
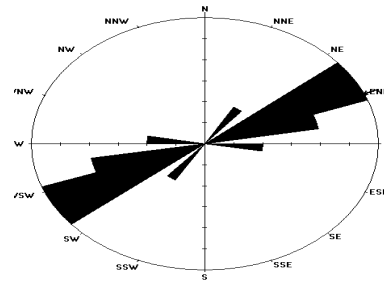


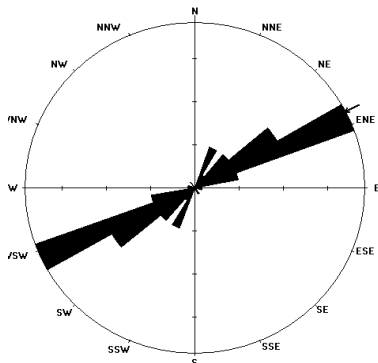
Figure 24: Lineament density map of the study area from aeromagnetic data



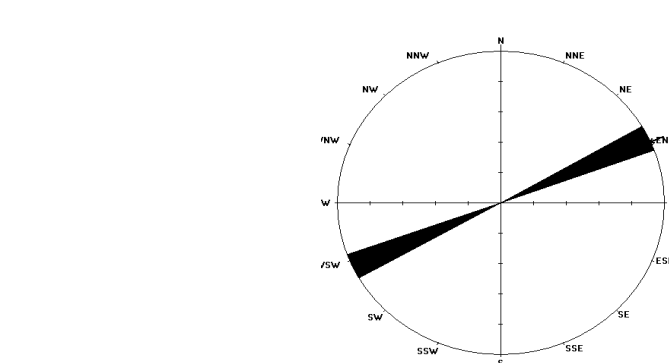
(a) Rose diagram plot for the extracted lineaments



(b) Rose diagram plot on granitic rocks



(c) Rose diagram plot for quartzites



(d) Rose diagram for Pegmatites & amphibolite greenschist

Figure 25a-d: Rose diagram plots for lineaments extracted from aeromagnetic data for each lithologic type in the study area (manually)

### **Geophysical Technique for Lineament Mapping**

Results of geophysical methods using aeromagnetic data were applied to be able to delineate the geology, structure, iron-bearing geologic bodies and lithological boundaries established within the study area. The airborne aeromagnetic data as a geophysical method generated high resolution maps that show major lithology and structural features in the area. The use of geophysical study approach is to delineate geological structures since mineralization can be structurally controlled in the study area. This data was an outcome of an aeromagnetic study carried out on the study area which lies within the Ilesha schist belt of the Southwestern Nigeria. The data was acquired by a magnetic equipment type known as the C.S.F Caesium Steamer on board a plane type 680 FL which was flown at a barometric altitude of 2600 m. The aeromagnetic survey carried out consist of flight lines-oriented NW-SE and spaced 3.5 to 4 km apart and transverse lines-oriented NE-SW with 10 to 15 km spacing. The entire aeromagnetic map sheet was scanned and the grids containing the sheets of the study area were extracted, scanned and digitized using ArcGIS software, then processed by applying several mathematical filters and transformation operators using Geosoft Oasis Montaj software (version 8.3) namely the horizontal gradient, Tilt-Derivative and Euler Deconvolution. The application of these filters have been so useful in the elaboration and production of several magnetic maps to include Total Magnetic Intensity (TMI), Upward Continuation, Residual Magnetic Anomaly, Horizontal Derivative along X, Y and Z directions, Total Horizontal Derivatives, Tilt Derivative, Analytical Signal, Reduction to pole, Reduction to Equator and other relevant maps required for the structural interpretation of the magnetic results.

### **Total Magnetic Intensity (TMI):**

The Total Magnetic Intensity (TMI) image of the study area was drawn on a scale of 1cm:2500m as the map is used to show variations in the magnetic intensity values of rocks in the study area. Areas with low magnetic intensity values exhibit high magnetic susceptibility hence hosting iron-bearing rocks depicted in blue colour. Area with high or very high magnetic intensity values have low magnetic susceptibility which are represented in pink colour. Total magnetic intensity level in the study area ranges from -140.8 to 258.3 nT, which suggests contrasting magnetic susceptibilities or variation in structural extends of the rock types in the investigated area. Low magnetic intensity values range from -140.8 to 38.0 nT which connotes high magnetic susceptibility. High magnetic intensity values range from 74.9 to 108.2 nT while very high magnetic intensity values range from 113.0 to 258.3nT. This geologically implies that areas appearing blue in colour with high magnetic susceptibility host iron-bearing rocks (Figure 26).

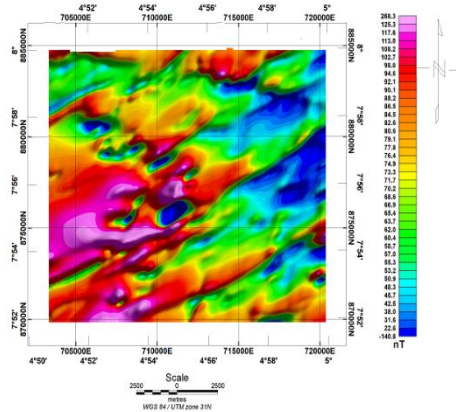


Figure 26: Total Intensity Map (TMI)

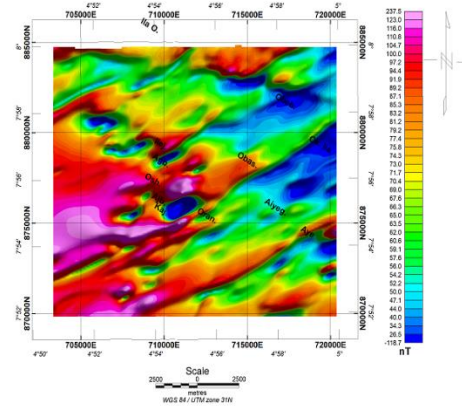


Figure 27: Reduction to the Equator Map (RTE)

### Reduction to the Equator (RTE)

Nigeria is located in the low magnetic region and close to the magnetic pole and too far from both the North and South to the pole. The need for carrying out reduction to equator or pole was to remove the magnetic field influence due to the dipping effect of the geologic bodies. The RTE map helps to remove the effects of magnetic inclination in the low magnetic latitude region by focusing the peaks magnetic anomalies over their sources and enhancing the basement architecture including structural lineaments with its orientations. Areas with magnetic susceptibility are identified around the northeastern, north central and minor cases spotted around the northwestern parts are dominated by high amplitude magnetic anomalies values ranging between 73.0 nT and 237.5 nT which is imminent around the western section of the area. While towards the southeastern part of the study area shown on the RTE map, the area is characterized by moderately low amplitude magnetic intensity values between 57.8 nT and 77.4 nT marked with greenish to light brown colours suggesting regions characterized by geological structures (fracture/fault) with low magnetic contents (Figure 27)

### Residual Magnetic Anomaly Map and Reduction to Pole

The residual magnetic field map highlights the existence of magnetic maxima and minima showing important variation of the magnetization in the subsoil with magnetic field values. The residual magnetic anomaly map of the study area illustrated that the dominant magnetic anomaly trends in the study are predominantly in the NE-SW direction (Figure 28). Magnetic lows were within high magnetic reliefs zones at various regions within the study area. In view of the low magnetic latitude of the study area, these magnetic lows are symptomatic of rocks with relatively higher magnetic susceptibility, a good case in point being the anomaly over the schist and amphibolites in the southwestern corner of the map. Reduction was made possible so as to eliminate the anomalies distortion caused by inclination of the earth's magnetic field (El Gout et al., 2009). Results from the Reduction to Pole show area of high magnetic susceptibility with low magnetic intensity values tilt towards the north pole. Areas of moderate magnetic susceptibility (appearing in green colour and yellow) share close boundary with regions of high magnetic susceptibility while areas of low or very low magnetic susceptibility

in reddish brown and pink colours occupy the western section (Northwestern and Southwestern) of the area. (Figure 29)

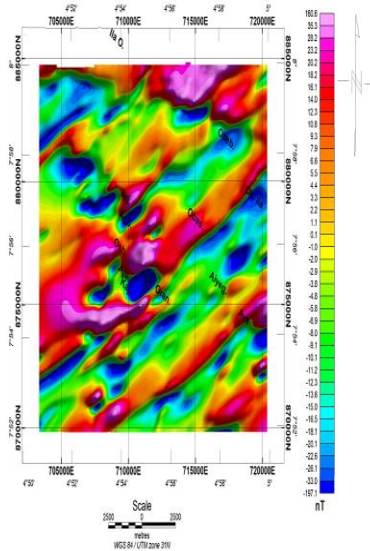


Figure 28: Residual Magnetic Anomaly Map

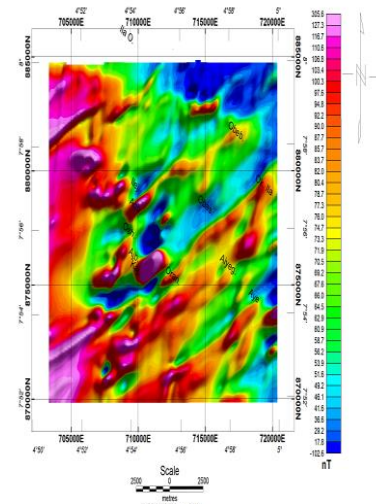


Figure 29: Reduction to Pole Map (RTP)

### Horizontal Derivatives Along X, Y and Z Directions

Horizontal derivative map along X-direction show elongated anomalies with the areas of high magnetic susceptibility dispersed across the entire section of the area as they also show common boundaries with areas of moderate and very low magnetic susceptibility. At the centre is a concentration of areas of high magnetic susceptibility showing close boundary with areas of very low magnetic susceptibility. Magnetic intensity values range from -0.4796 to 0.2930 nT. Horizontal derivatives along Y direction also show elongated 2D anomalies trending in a preferred direction towards the NE-SW. The high magnetic susceptibility areas were also seen to be displayed and showing close boundaries with areas of moderate and low magnetic susceptibility. However, there is a cluster or concentration of the areas of high magnetic susceptibility towards the centre showing close boundary with areas of moderate magnetic susceptibility with the least magnetic intensity value being -0.6420nT and the highest being 1.1801 nT. Along the Z direction is an even spread of the areas of low, moderate and high magnetic susceptibilities which are displayed in a manner that they show elongated geologic boundaries. The least magnetic intensity value is -1.0408 and the highest magnetic intensity value is 1.0661nT. Geological structures were well delineated at the NE-SW direction which might be considered as the representation of fault or fracture (Figure 30).

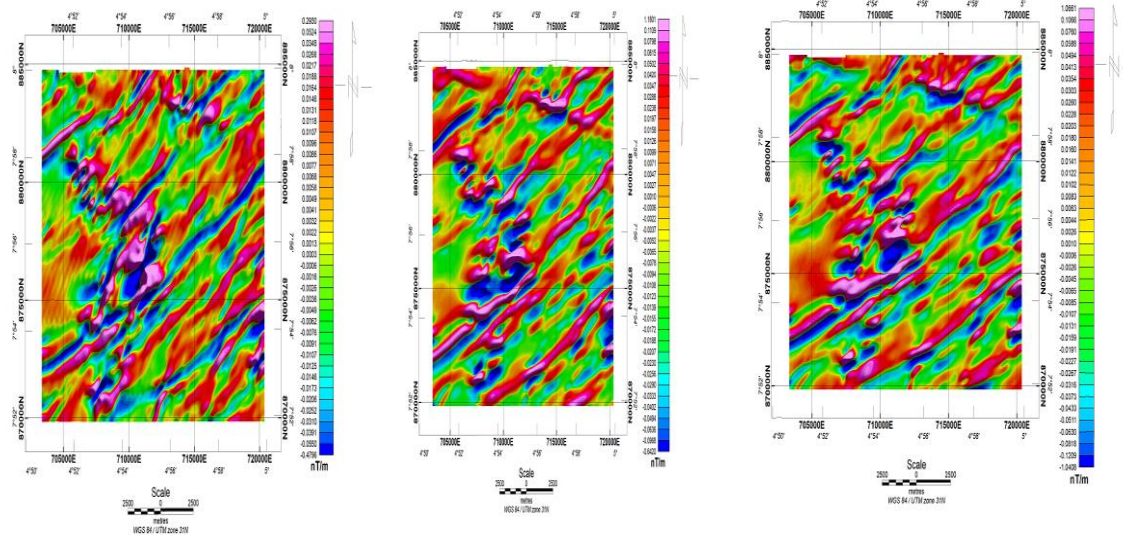


Figure 30: Horizontal Derivatives along X, Y and Z respectively

### Total Horizontal Derivative (THD)

Total horizontal derivative filter is an effective tool in detecting edges of magnetized structures in the region and accentuate shallow anomalies. Total horizontal derivative map was generated from the aeromagnetic data in order to enhance the anomaly curvature of the near-vertical structures arising from the changes of contrasting magnetic susceptibility. Magnetic intensity value for the total horizontal derivative ranges from 0.000nT to 1.2584nT. Consequently, structural features and boundaries of causative sources can be enhanced. Prominent structurally trend in the NE – SW as conspicuously observed on the map (Figure 31a).

### Tilt Derivative (TD)

Tilted at angle of inclination to be able to see the direction in which the linear features and geologic bodies within the study area are trending. However, areas appearing in blue colour are inclined at an angle between -71.2 to -90 degrees which are noted to be the area with high magnetic susceptibility. The geologic bodies and linear features are seen to elongated and all trending in the NE direction. Areas with very low magnetic susceptibility are seen to trend or be orientated between 70.1 to 90 degrees. Summarily, the entire linear features are seen to trend between -90 and 90 degrees (Figure 31b).

### Analytical Signal

Analytical signal amplitude ranging between 0.0006 to 1.1862nT/m. Geologic bodies with high magnetic susceptibility record the peak of their signals ranging between 0.0006 to 0.0122nT/m. Geologic bodies with moderate magnetic susceptibility appearing in green record signals with their peaks ranging between 0.0207 to 0.0338nT/m while geologic bodies with low to very low magnetic susceptibility have the peaks of their signals ranging between 0.0426 to 1.1862nT/m. Hence, signals obtained from the results of the analytical signals have their peaks range between 0.0006 to 1.1862nT/m (Figure 31c).

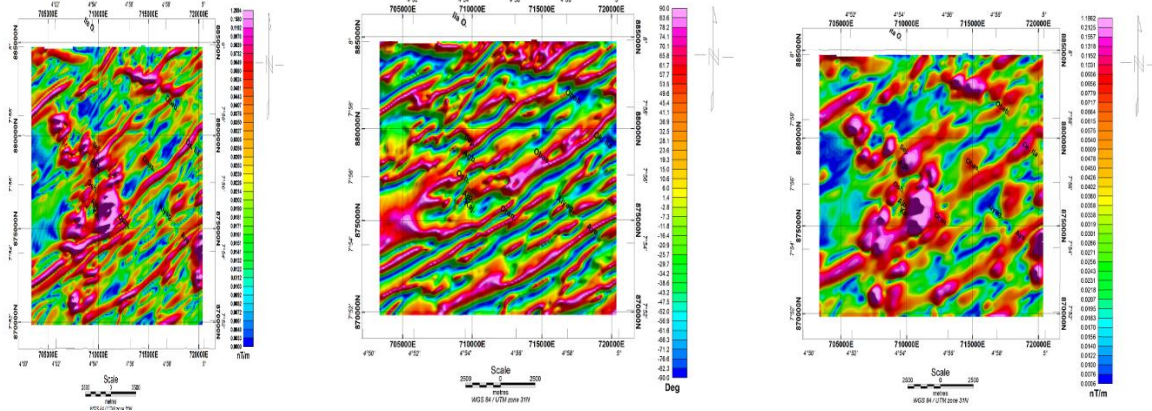


Figure 31a-c: Total Horizontal Derivative, Tilt Derivative and Analytical Signal respectively

### Euler Deconvolution

From the Euler deconvolution map, the depths at which the linear structures or features are encountered are shown as some of the linear features which are mapped structures can either occur as shallow or deep-seated features. Deep seated features are picked at a depth greater than 600m and those that exist at a depth ranging between 300m to 600m. However shallow seated linear features were encountered at a depth less than 300m. Linear features appearing in blue are encountered at a shallow depth less than 300m. Features in red were encountered at a depth between 300m to 600m while only few of these features were captured at a depth greater than 600m which are described as deep-seated structures. The magnetic susceptibility of the geologic bodies ranges between -197.1nT to 160. 5nT. The extracted lineaments reflect the position of features such as fault, deep fractures and geologic contacts within the study area as revealed from aeromagnetic data acquired (Figure 32a-c).

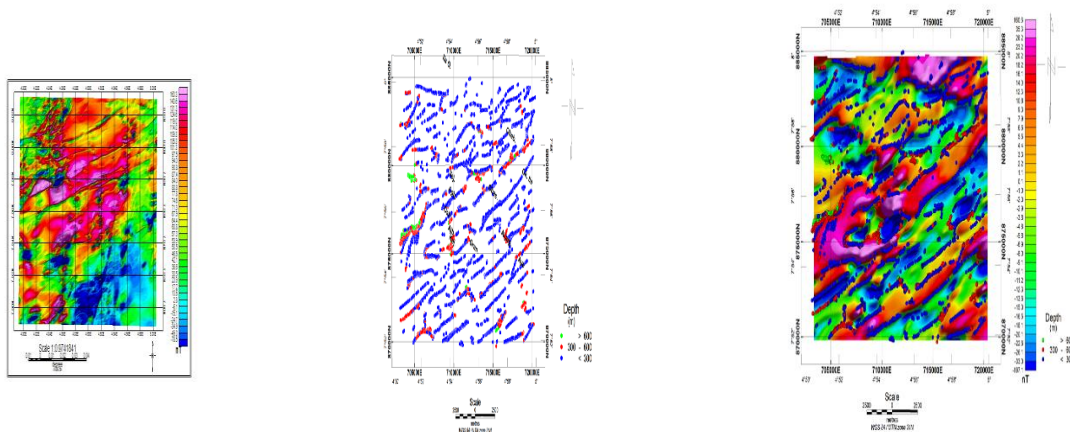


Figure 32a-c: Upward Continuation, Euler Deconvolution and Euler Solution Superimposed Maps

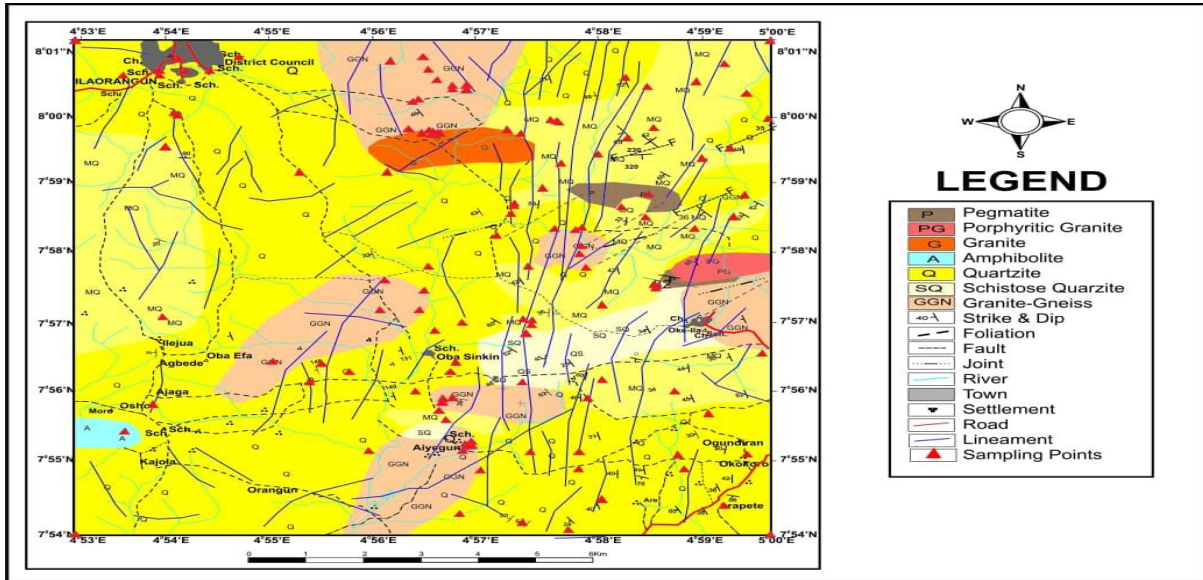


Figure 33: Lineaments extracted from Landsat-8 OLI imagery superimposed on the geological map of the area

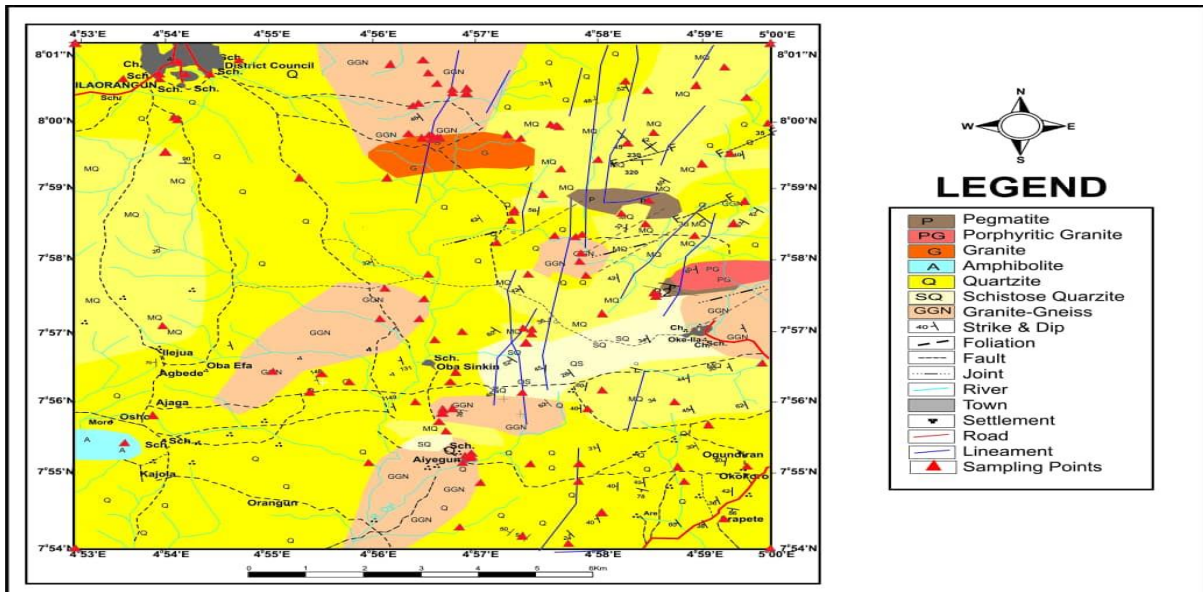


Figure 34: Lineaments extracted from SRTM imagery superimposed on the geological map of the study area

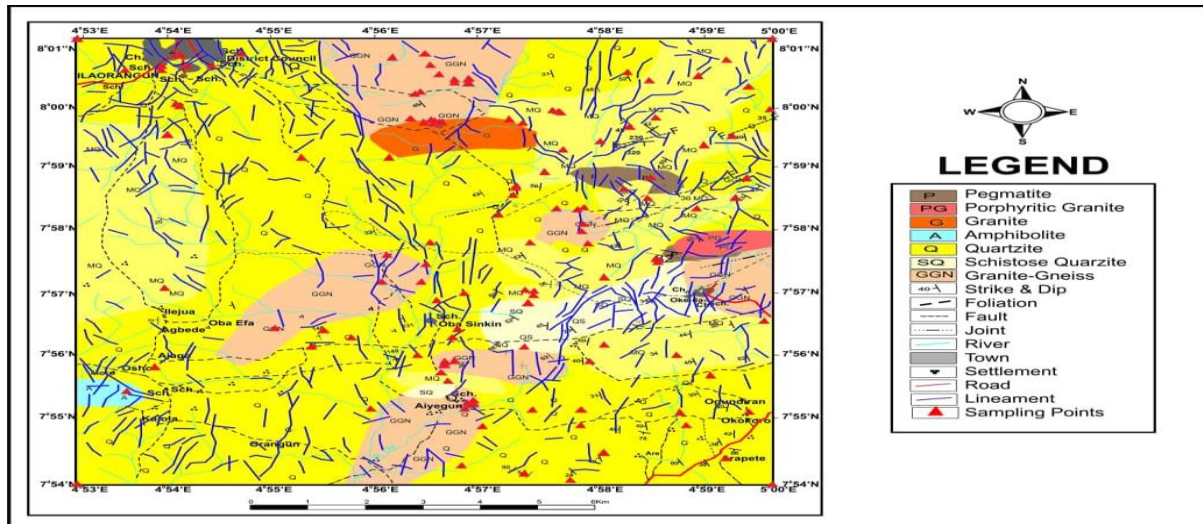


Figure 35: Lineaments extracted from Radar Sentinel-2A imagery superimposed on the geological map of the area

Details of lineaments extracted from Landsat -8 OLI (Figure 33), SRTM and Radar Sentinel-2A when superimposed on the geological map of the study area revealed that lineaments were superimposed on the geological map of the study area so as to infer which lithology or rock type is most deformed. The cluster and density of lineaments on the quartzite lithology is as a result of the brittle nature of quartzites. Hence, tends to respond to the effect of deformational processes. It is clearly observed that the eastern section of the study area is the most deformed and affected by the orogenic episodes. Hence, a potential mineralization zone is established in the eastern section (NE & SE) of the study area. Despite the few lineaments extracted using the SRTM remote sensing tool, the few available or captured lineaments are only visible on the eastern section of the study area (Figure 34). Clearly justifies that part of the study area as a potential mineralization zone. Presence of lineaments in the eastern section of the study area was made possible because of the brittle nature of the underlying lithology of the area identified from ground truthing as quartzites. When superimposed on the geological map revealed a large population of lineaments captured across the entire area. However, there are visible cluster of lineaments of varying lengths forming T-crossing or X-crossing relationship on the eastern section of the study area. Orientation of lineaments within the area from the Radar Sentinel show lineaments of multi directional trends as they trend in the NE-SW, NW-SE directions. While subsidiary lineaments were seen trending in the N-S and E-W directions (Figure 35). Potential mineralization zones were spotted in the eastern section of the study area. Comparing lineaments extracted from the Landsat -8 OLI, SRTM and Radar Sentinel-2A and superimposed on the geological map of the area, the mineral occurrence in the area is predicted to have been structurally controlled. In summary for all the remotely sensed satellite imageries produced Landsat -8 OLI, SRTM and Radar Sentinel -2A. Result showed that 80% of the lineaments captured from the remotely sensed satellite imagery were found on the quartzites while the remaining 20% were found on other rock types which include granite gneiss, pegmatites and amphibolites green schist. Quartzite lithology being the most dominant, existing as either schistose or massive are brittle in nature hence prone to respond to deformational or orogenic



activities and are possible mineralization zones. The eastern section suggests a possible hot spot for mineralization in the study area from potassium radiometric anomaly map produced. For the possibility of mineral exploration in the study area, the analysis of potassium concentration from radiometric data acquired for the study area was carried out with the aim of identifying the possible pattern of mineralisation which may be associated with gold and other metallic minerals deposition in host rocks within the area. This geophysical method was also employed to spot and pick hydrothermalised zones pertinent to known gold and heavy metallic minerals mineralisation within the area. From interpretation, high potassium deviation (KD) anomaly values range between 1.3 to 2.1 % with the dominant lithology being quartzites with pegmatite intrusions. Moderate potassium deviation (KD) anomaly values range between 0.6 to 1.2% with dominant lithologies being quartzites and granite gneiss while low potassium deviation (KD) anomaly values range between 0.2 to 0.5% which are found on almost all the lithologies mapped within the study area. Cases of very low potassium deviation (KD) anomaly values range between 0.1 to 0.2%. High potassium (KD) anomalies denoted by 'H' were interpreted as hydrothermal alteration zones suggesting zones within the area with the possibility of gold mineralisation, sulphide mineralisation and some heavy metals which are pathfinder elements to gold mineralisation in the study area.

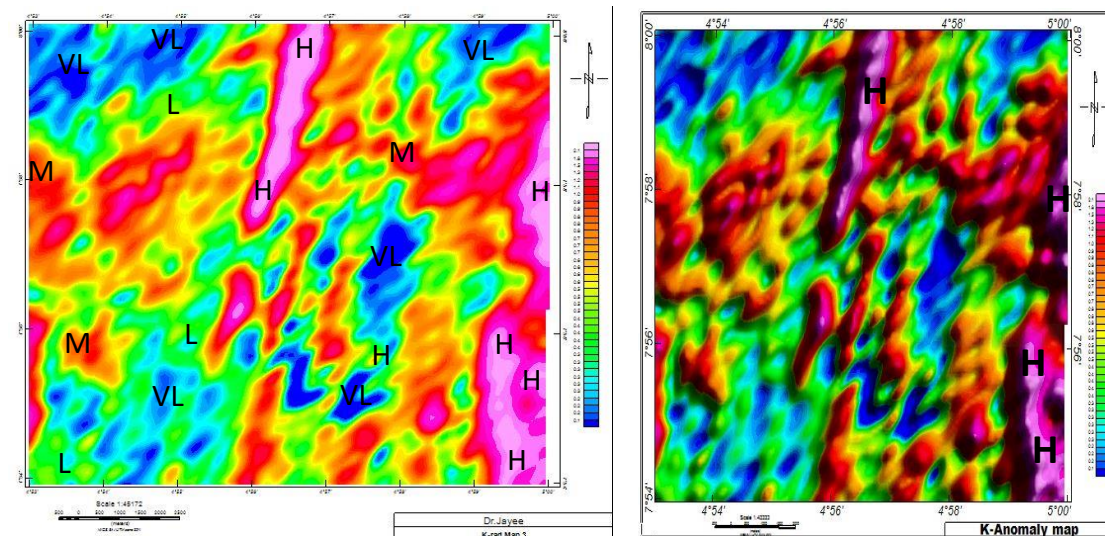


Figure 36: Potassium radiometric anomaly map of the study area in plain and 3D Imageries

## CONCLUSION AND RECOMMENDATION

From the research, which adopted an integrated study approach involving the use of remote sensing and geophysical methods for the purpose of litho-lineament mapping of basement rocks in Ila Orangun area, the researcher therefore deem it fit to conclude that remote sensing techniques used which combines Landsat-8, SRTM, Radar Sentinel-2A and geophysical methods such as the Aeromagnetic data were all found useful in the recognition and mapping of lineaments which represent large scale structures suspected to have played vital role in the

possible occurrence of minerals which are predicted to be structurally controlled. The general orientation and trend of the lineaments in the study area from all the lineament maps produced using the Landsat-8, SRTM, Radar Sentinel -2A and Aeromagnetic data show majority trending NE-SW and a few trending in the N-S and E-W directions. The eastern sections (northeastern and southeastern) of the area around Obasinkin, Aba Aromodana, Aba Jagi, Aba Agbonore, Aba Obalumo and Oke Ila are observed to host rocks identified to be the most deformed as they are characterised with heavy presence of foliations, fractures, joints, faults and folds delineated as lineaments. The lineament density is however connected with the brittle nature of quartzites in this part of the study area. Hence, identified as a possible mineralization zone. The researcher recommends that similar or related geological studies using same integrated study approach should be conducted on neighbouring localities to Ila Orangun specifically around Igbomina communities in the southwestern Nigeria for possible comparative studies.

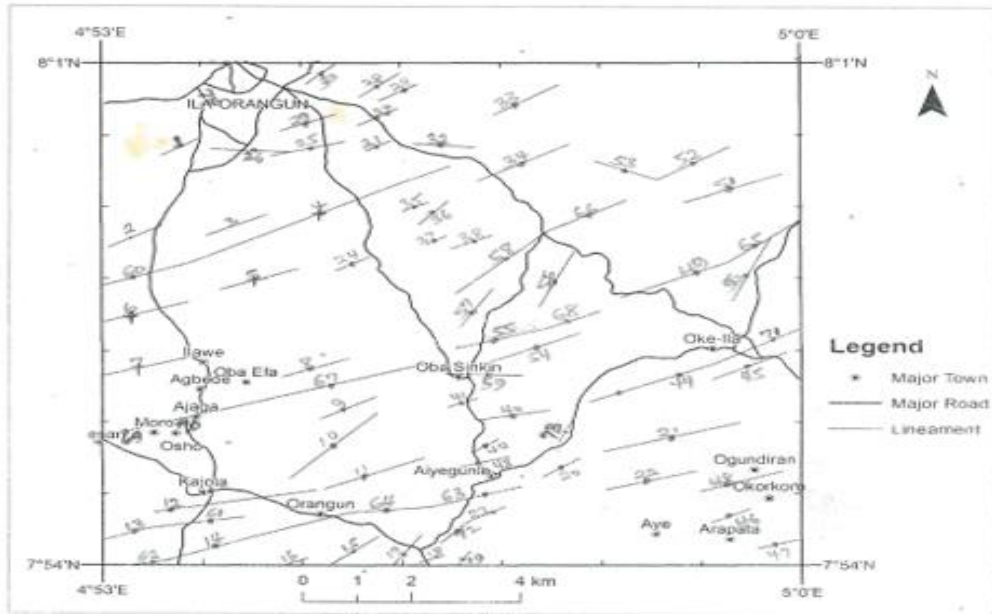
## REFERENCES

- Annor A.E. 1998. Structural and Chronological Relationship Between the Low Grade Igarra Schist and Its' Adjoining Okene of Southwestern Nigeria. *Journal of Mineral Geology volume 34, Issue 2, pp. 187-196*
- Arlegui L.E. and M.A. Soriano 1998. Characterizing Lineament from Satellite Images and Field Studies in the Central Ebro Basin, NE Spain. *International Journal of Remote Sensing volume 19, pp. 3169-3185*
- Ayodele O.S. 2010. Analysis of the Lineament Extracted from Landsat Image of Okemesi Area, Southwestern Nigeria. *India Journal of Science and Technology, volume 3, pp. 31-36*
- Ayodele O.S. and Odeyemi I.B. 2010. Analysis of the Lineaments Extracted from Landsat TM Image of the area Around Okemesi, Southwestern Nigeria. *In Indian Journal of Science and Technology, volume 3, Issue 1, ISSN 0974-6846, pp.31-36*
- Blenlincop T.G and Rutter E.H 1956. Cataclastic Deformation of Quartzite in the Moine-thrust Zone: *Journal of Structural Geology volume 8, pp. 669-681*
- Boadi B. 2013. Geological and Structural Interpretation of the Korongo Area of the Ancient Gold Belt of Ghana from Aeromagnetic and Radiometric Data. *International Research Journal of Geology and Mining, volume 3, pp. 124-135*
- Boesse S. and Ocan. O. 1992. Geology and Evolution of the Ile-Ife Ilesha Schist Belt, Southwestern Nigeria. *In Benin Nigeria Geo-Traversal International and Tectonics of High Grade Terrain. IGCP 215, pp.123-129*
- Drury 1992. Tectonothermics of Modern and Ancient Continental Margins. Published *In Book; Basement Tectonics. vol. 8 pp. 27- 36.*
- Edet A.E et al., 1994. Lineament Analysis for Groundwater Exploration in Precambrian Oban Massif and Obudu Plateau, SE Nigeria. *In Journal of Mining and Geology. volume 30, Issue 1, pp. 81-85*
- Ekwueme B.N. 1987. Structural Orientation and Precambrian Deformation Episode of Uwet area. Oban Massif SE Nigeria. *Precambrian Resources volume 34, pp. 269-289*

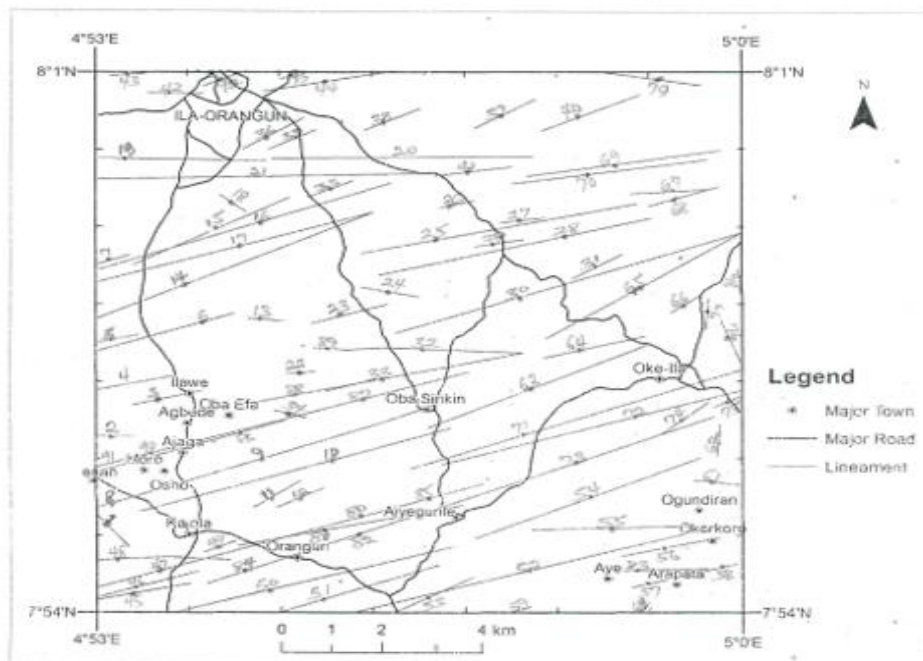
Publication of the European Centre for Research Training and Development -UK

- Fagbohun B.J et al., 2017. Integrating GIS and Multi-Influencing Factor Techniques for Delineation of Potential Ground Water Recharge Zones in Part of Ilesha Schist Belt, Southwestern Nigeria. *Environment Earth Sciences*, volume 77, pp.
- Fagbohun B.J. et al., 2017. Lithostructural Analysis of Eastern Part of Ilesha Schist Belt, Southwestern Nigeria. *Published in Journal of African Earth Sciences. Volume 133, pp.123-137*
- Fernandez M.T. et al., 2001. Hydrothermal Alteration and Main Structures Mapping Using TM Images in La Primavera Geothermal Field Mexico. *Published in Geofisica International, Volume 40, Issue 3, pp.147-162*
- Gaafar I.M. 2016. Integration of Geophysical and Geological Data for Delineation of Mineralized Zones in Umnaggat Area, Central Eastern Desert, Egypt. *NRIAG Journal of Astronomy and Geophysics, volume, pp. 86-99*
- Johnson S.Y and Watt J.T 2012. Influence of Fault Trend, Bands and Convergence on Shallow Structure and Geomorphology of the Hosgri Strike - slip Fault, Offshore Central California: *Geosphere, volume.8, 25p.*
- Julius O.F. and Adekunle O.T. 2015. Evaluation of Terrain Conditions in Ilesha Schist Belt Areas, Southwestern Nigeria, Using Remotely Sensed Data. *In World Scientific News. Volume 19, EISSN 2392-2192, pp.69 -79*
- Kalinowski A.A. and Oliver S. 2004. ASTER Processing Manual, Remote Sensing Application, Geo-Science Australia, Internal Report 39 pp
- Odeyemi I. B. 1988. Lithostratigraphic and Structural Relationships of the Upper Precambrian Metasediments in Igarra Area, Western Nigeria. *The Precambrian Geology of Nigeria, Geological Survey of Kaduna, pp. 111-123*
- Odeyemi I.B. 1988. A Review of Orogeny Events in the Precambrian Basement of Nigeria, West Africa. *In Geologic Rundschau, volume 70, Issue 3, pp. 897-909*
- Odeyemi I.B. 1993. A Comparative Study of Remote Sensing Images of Structure of the Okemesi Fold Belt, Nigeria. *Journal of volume 1, pp.77- 83*
- Oluyide P.O. 1998. Structural Trends on the Nigerian Basement Complex. *In Precambrian Geology of Nigeria. Geological survey of Nigeria. pp. 95-98*
- Omitogun A.A. and Ogbole J.O. 2017. Lithologic, Hydrothermal Alteration and Structural Mapping of Okemesi Folds and Environs Using Landsat 8 OLI and ASTER DEM. *In Journal of Geography, Environment and Earth Science International. Volume 12, Issue 3, pp.1-19*
- Rahaman M.A. 1976. Review of the Basement Geology of SW Nigeria. *In Geology of Nigeria. Elizabeth Publishing Company Nigeria, pp.41-58*
- Urai J.I et al 1991. Lineaments of Crystal Growth in Synthetic Fibrous Vein. *Journal of Structural Geology volume. 13, Issue 1, pp. 823-836*

**APPENDIX**



a: Lineaments extracted manually from aeromagnetic data (Total of 74 Lineaments)



b: Lineaments extracted automatically from aeromagnetic data (Total of 93 Lineaments)

### **FUNDING SOURCE**

This research was fully funded by the Tertiary Education Trust Fund (TETFund) Nigeria. This research article is the outcome of a research work carried out by the corresponding author and the co-authors which got full funding from the above-mentioned government agency established by an act of the Federal Government of Nigeria.

### **ACKNOWLEDGEMENT**

I acknowledge the efforts of Dr. Awoniran and Mr. Oyebolu for assisting the researchers with relevant software packages and remote sensing tools that were used in the remote sensing aspect of this research. Their contributions towards the making of this research work is highly appreciated.

### **Authors Contribution**

The corresponding author and the co-authors initiated the research and embarked on the field work with the mission of ground truthing. The co-authors provided guidance where needed in the writing of this manuscript. However, manuscript writing was done by the corresponding author.

### **Conflict of Interest**

There is no conflict of interest as both the corresponding author and co-authors are in agreement to submit the full manuscript of the outcome of this research to your journal for publishing.